

## GEOTECHNICAL CHARACTERIZATION OF FUCINO CLAY

A.G.I. - ASSOCIAZIONE GEOTECNICA ITALIANA <sup>1</sup>

<sup>1</sup> This paper is the result of the close cooperation of a study group promoted by A.G.I. and formed by: A. BURGHIGNOLI, L. CAVALERA, V. CHIEPPA, M. JAMIOLKOWSKI, C. MANCUSO, S. MARCHETTI, V. PANE, P. PAOLIANI, F. SILVESTRI, F. VINALE, E. VITTORI

**ABSTRACT:** The paper represents a joint effort of a number of Italian research groups in the attempt to characterize a thick deposit of the soft, homogeneous highly structured  $\text{CaCO}_3$  cemented Fucino lacustrine clay. The paper focuses mainly on the stress history, compressibility and stiffness characteristics of the deposit to fit with the general theme of the Conference. A comprehensive series of laboratory and in situ tests have been performed. The results of these tests have been critically evaluated and have led to a detailed geotechnical characterization of the tested clay and have allowed some relevant remarks on the use of in situ techniques in structured clays.

**RESUME:** Le texte est le résultat de l'effort commun de quelques groupes de chercheurs italiens pour caractériser une couche épaisse d'argile molle, homogène, cimentée par  $\text{CaCO}_3$  et hautement structurée, qui appartient au bassin du lac Fucino. En accord avec le thème général de la conférence, le rapport est centré sur les paramètres qui concernent l'histoire tensionnelle, la compressibilité et la compacité de la couche. On a exécuté nombre d'essais de laboratoire et in situ, dont on a interprété et évalué critiquement les résultats à fin de dériver une caractérisation géotechnique détaillée. L'étude a conduit aussi à des importants remarques sur l'emploi des essais in situ dans les argiles structurées.

### 1 INTRODUCTION

In 1986 the Department of Structural and Geotechnical Engineering of the University of Rome La Sapienza has undertaken a research grant with the Italian National Agency for Alternative Energy Sources (ENEA); the primary purpose of the research was to select a testing site, and to provide its geotechnical characterization with regard to static and dynamic loading conditions. The related field and laboratory investigations have been carried out by means of a joint effort of the Universities of Napoli, L'Aquila, of Texas at Austin, of the Technical University of Torino, with the support of ENEA and ISMES personnel.

The selected site is constituted by a deep clayey deposit of lacustrine origin located in the Fucino basin, about 80 km east of Rome.

The experimental activity, which lasted more than two years, has been documented in several research reports and publications. In the following it is presented a synthetic description of the laboratory and field tests with particular emphasis on the deformability characteristics of the clay, aimed at providing the scientific community with an example of an unusually comprehensive and detailed geotechnical investigation.

### 2 GEOLOGY

The Fucino basin is a wide intramountain depression (about 1000 km<sup>2</sup>) within the central Apennines, surrounded by high mountains of mesozoic-cenozoic carbonatic rocks. Once the basin hosted a wide lake, which was artificially drained in the last century for land reclamation.

Fine lacustrine and coarse alluvial deposits fill the basin with a thickness locally in excess of 1000 m. The sedimentary record shows that for long time spans during the Quaternary (last 1.8 million

years) this basin had no outlets and the lake shores reached heights up to many tens of meters above the historical elevation (posed at about 660 m above sea level).

As recent studies indicate, the tectonic origin of the Fucino depression is shown by the normal faults bounding its edges. The Serrone fault, on the southeastern flank, was reactivated in 1915, when a strong earthquake (Richter magnitude 6.8) hit the area causing considerable damage (Serva et al. 1986). In addition, surface faulting has been outlined on aerial photos and satellite images (Giraudi 1988), thus suggesting that other similar seismic events have occurred in the past.

The investigated area borders the most depressed zone ("Bacinetto") at about 650 m above sea level. Along the investigated stratum, (40 m) the sediments are lacustrine clays, without any significant variation in grading; on the contrary, the calcium carbonate ( $\text{CaCO}_3$ ) content varies considerably with depth. The comparison between the trend of the  $\text{CaCO}_3$  content profile and the palinologic data, reported in Follieri et al. (1986), suggest a strong influence of the global climatic changes whose ages can be well estimated; this provides an indirect way for dating the stratigraphic profile. The following sedimentation rates can be assessed:

Depth	Age	Sedimentation	Period
[m]	[yr]	Rate [mm/yr]	
0-6	0-13000	0.46	Holocene
6-24	13000-32000	0.95	Würm
24-40	32000-64000	0.50	Würm interglacial

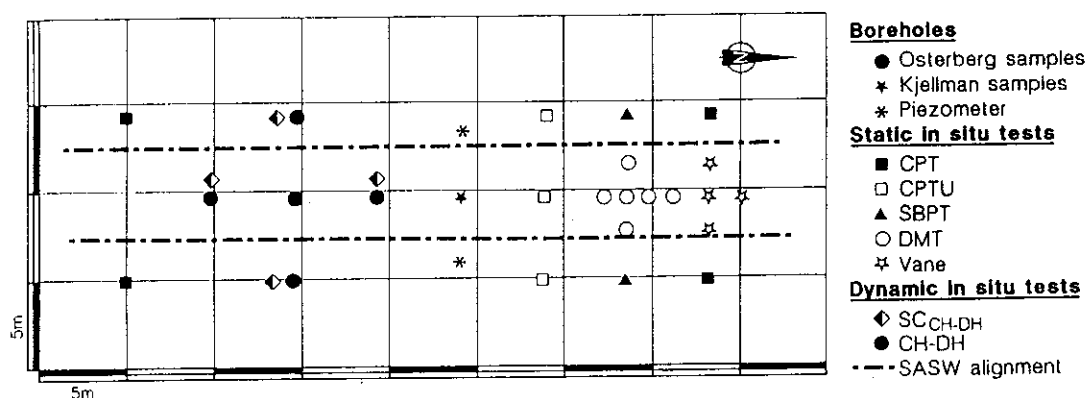


Figure 1. Lay-out of investigation program.

### 3 INVESTIGATION PROGRAM AND BASIC SOIL PROPERTIES

The primary purpose of this study was to provide a comparison among results of various field and laboratory tests. In order to minimize the influence of spatial variability of physical, chemical and mechanical properties of the clay under investigation, the attention has been focused on a relatively small volume of soil, having plan dimensions of  $10 \times 40 \text{ m}^2$  and thickness of about 40 m. The area pertaining to the investigation program and the locations of the boreholes and field tests are shown in Figure 1.

A considerable number of undisturbed samples was collected by means of an Osterberg (1973) piston sampler. In addition, continuous Kjellman samples were collected in order to provide a detailed examination of the macro-structural characteristics of the deposit. Standard laboratory tests have been carried out on the undisturbed samples, together with simple shear (DSS-CKoU) tests and cyclic torsional shear tests.

In order to appreciate the degree of homogeneity of the area under study, it is sufficient to examine the four static penetration tests, performed at the corners of the area and collected in Figure 2. The profiles shown in this figure reveal a fair homogeneity, both in vertical and horizontal directions; the soil stratigraphy is virtually identical at the 4 test locations, with thin sandy layers being identified at the same depth by all tests.

The upper part of the deposit, down to a depth of a few meters, has been subjected to overconsolidation due to dessiccation and groundwater level fluctuations. During the whole duration of the field investigation program (May-July 1987), piezometric measurements have shown a hydrostatic pore pressure distribution, and a water table located about 1 m below ground surface.

General characteristics and index properties of Fucino clay are shown, as a function of depth, in Figure 3. The values of the natural moisture content,  $w$ , range between 60 and 120 %. The scatter is marked even within a single sample; as an example, Figure 4 shows the variation of  $w$  along an undisturbed sample (recovered at a depth of 15 m) where  $w$  ranges between 65 and 95 %; significant scatter is evident also in the central portion of the sample which, presumably, is the least affected by disturbance and drying.

As far as Atterberg limits are concerned, it is worth to note the particularly high values of  $w_L$  (between 90 and 120 %) below a depth of approximately

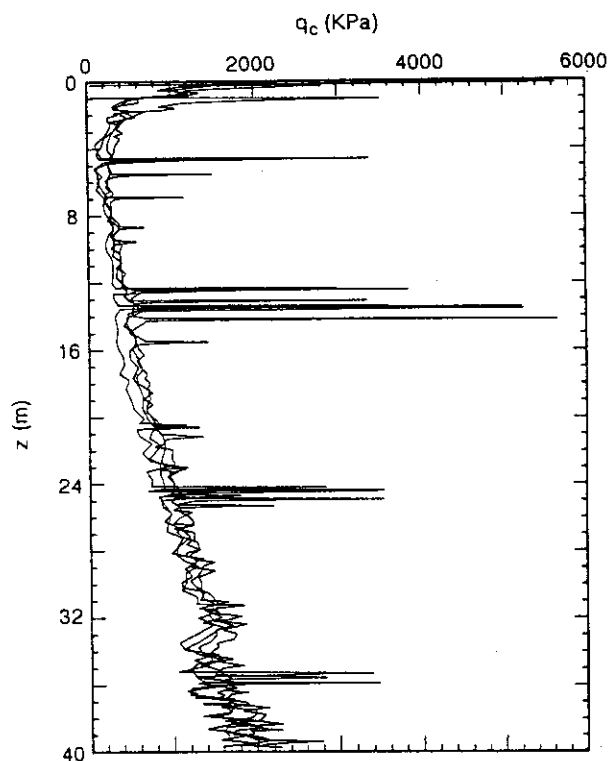


Figure 2. Static cone penetration test results.

10 m. On a plasticity chart, shown in Figure 5, the clay plots as an organic clay of high plasticity. It is worth to mention that this occurs despite the high calcium carbonate content. Activity is medium to high, ranging between 1 and 2.5.

As mentioned, the variation of calcium carbonate content is significant; in the upper 25 m of the deposit, the  $\text{CaCO}_3$  content is between 10 and 30 %; below this depth there is a marked increase, with an average value of about 60 %. The effects of  $\text{CaCO}_3$  content on the mechanical characteristics of the clay will be discussed in the following sections.

### 4 STRESS HISTORY

An attempt to evaluate the stress history of the clay deposit under examination is made with reference to the results of the following available laboratory and in situ tests:

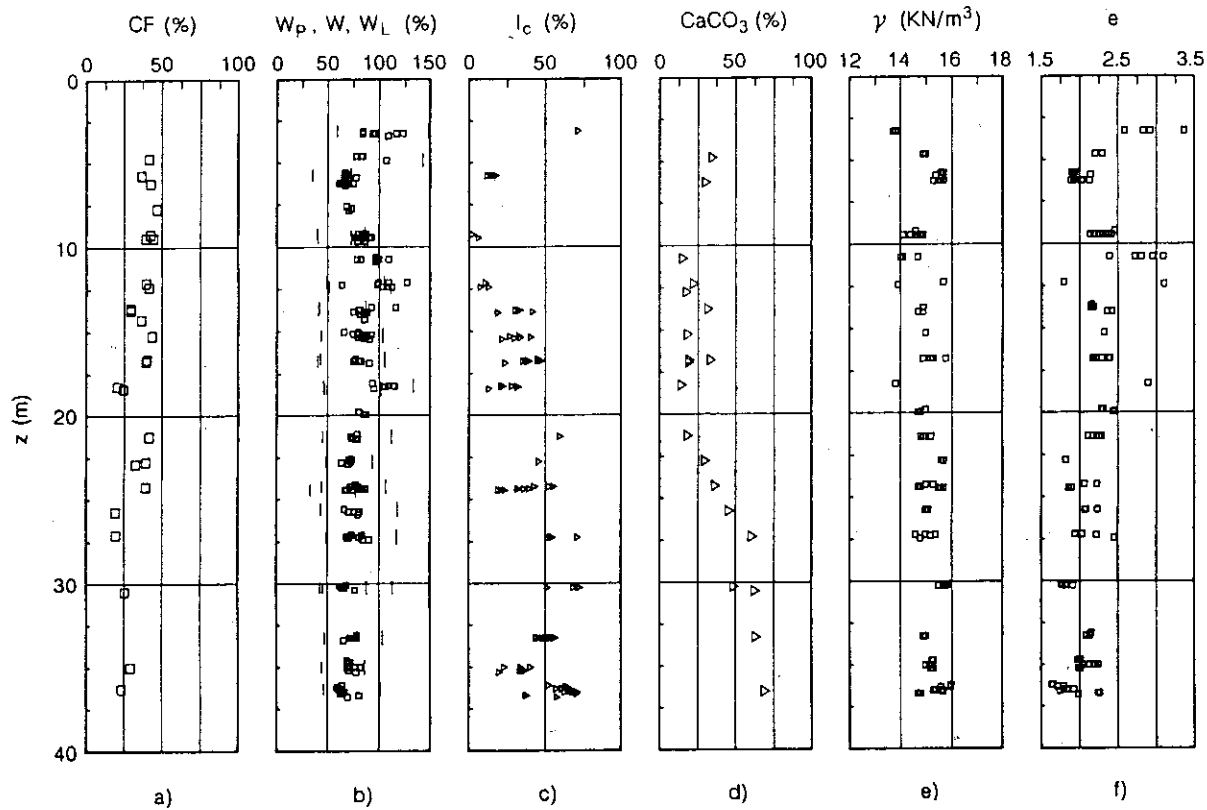


Figure 3. Index properties of Fucino clay.

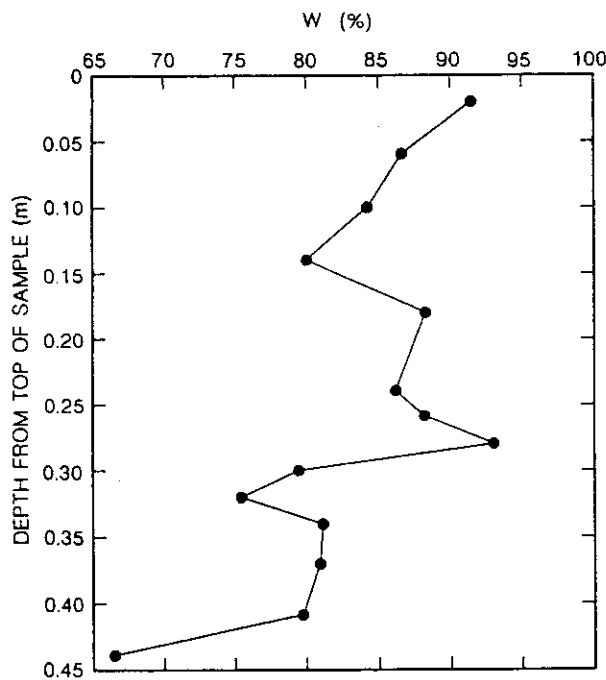


Figure 4. Natural water content within an undisturbed sample.

#### 4.1 Laboratory tests

The preconsolidation pressure  $\sigma'_p$  and the overconsolidation ratio  $OCR = \sigma'_p / \sigma'_{vo}$  have been evaluated on the basis of the results of both incremental loading (IL) and constant rate of strain (CRS) oedometer tests. For the IL tests, reference has been made to

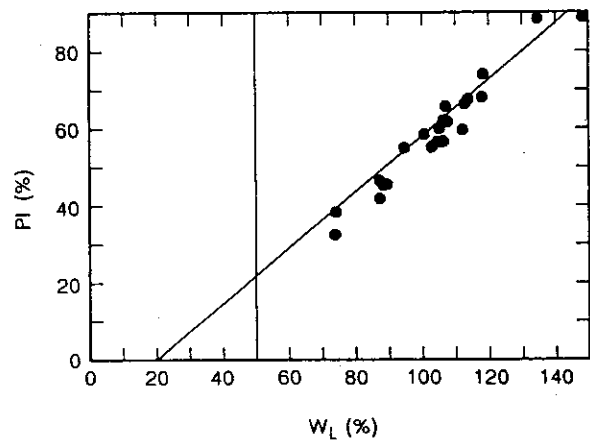


Figure 5. Plasticity chart.

the compression curves corresponding to the deformation attained after 24<sup>h</sup> of load increment. The values of  $\sigma'_p$  and OCR resulting from the analysis of oedometer tests, together with the calcium carbonate content, are reported in Figure 6.

#### 4.2 In Situ Tests

The results of in situ tests have been used to assess the coefficient of earth pressure at rest  $K_0$  and OCR. More specifically:

– The results of the Camkometer self-boring pressurometer tests (SBPT) allow to assess the values of

$$K_0 = \frac{p_0 - u}{\sigma'_{vo}} \quad (1)$$

where:

$p_o$  = total lift-off stress, resulting from the visual inspection of the early part of the expansion curve (Ghionna et al. 1981);

$u$  = pore pressure acting at the mid-height of the pressuremeter probe, here assumed equal to the hydrostatic one,  $u_o$ .

- The results of Marchetti's flat dilatometer tests (DMT) have been used to assess both OCR and  $K_o$  following rigorously the procedure suggested by Marchetti (1980).

- The results of field vane tests (FVT) performed with the "standard" blade have been used to estimate the order of magnitude of OCR using the following empirical expression:

$$\frac{c_u}{\sigma'_{vo}} = \left[ \frac{c_u}{\sigma'_{vo}} \right]_{NC} \cdot (OCR)^n \quad (2)$$

where:

$\frac{c_u}{\sigma'_{vo}}$  = normalized undrained shear strength obtained from the tests;

$\left[ \frac{c_u}{\sigma'_{vo}} \right]_{NC}$  = normalized undrained shear strength in normally consolidated state for completely destructured material, here assumed equal to 0.30;

$n$  = an exponent, that in cemented highly structured clays ranges between 0.9 and 1.1 (Jamiołkowski et al. 1985)

The information obtained from in situ tests is reported in Figure 7.

#### 4.3 In situ versus laboratory stress history

Based on the available geological information and considering the results displayed in Figures 6 and 7, the following comments can be made with regard to the stress history of the deposit:

a. Both laboratory and in situ tests results indicate that Fucino clay is lightly overconsolidated.

b. Based on the available geological evidence, this overconsolidation can be mainly attributed to structure, and in particular to secondary consolidation and post-depositional diagenetic bonds caused by  $CaCO_3$  cementation. In the upper part of the deposit (4 to 6 m), the groundwater level oscillation might have influenced the current stress history.

c. Given the dominant preconsolidation mechanisms, only aging could have resulted in an increase of  $K_o$  above the value corresponding to a destructured normally consolidated state,  $K_o^{NC}$  (Kulhawy et al. 1989). The results of an instrumented oedometer test have furnished  $K_o^{NC} = 0.64$ ; hence values of  $K_o \geq 0.85$  are difficult to be justified. A rough estimate of the influence of aging on  $K_o$  and OCR values may be obtained referring to the following expressions suggested by Mesri (1987 and 1989):

$$OCR_\alpha = \left( \frac{t}{t_p} \right)^{\beta_1} \quad (3)$$

$$K_{o\alpha} = K_o^{NC} \left( \frac{t}{t_p} \right)^{\beta_2} \quad (4)$$

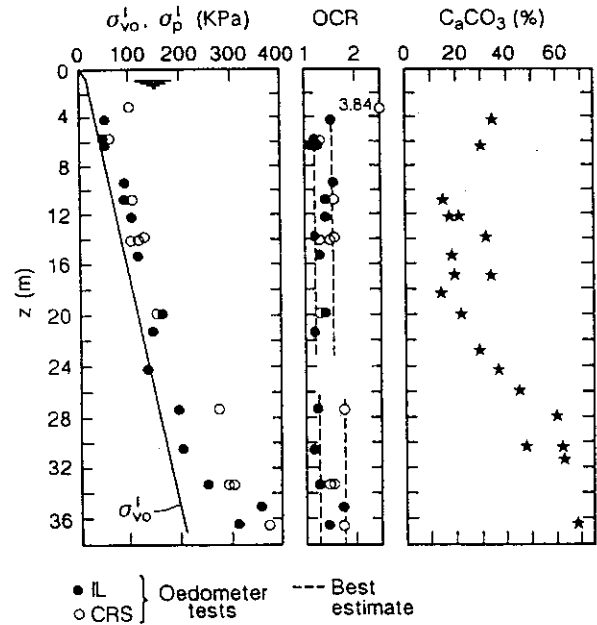


Figure 6. Stress history from laboratory tests.

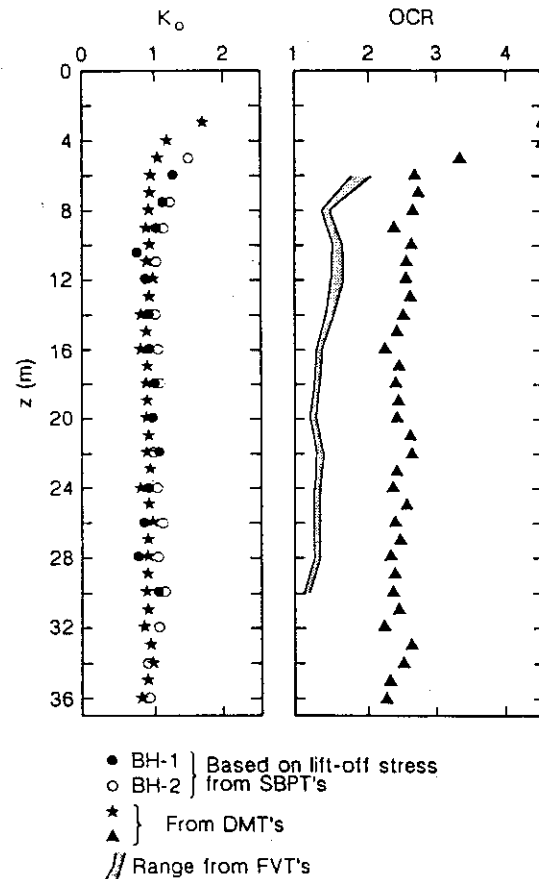


Figure 7. Stress history from in situ tests.

where:

$OCR_\alpha$  = overconsolidation ratio due to aging;

$K_{o\alpha}$  = coefficient of earth pressure at rest of aged NC clays;

$t_p$  = time at the end of primary consolidation;

$t$  = any time higher than  $t_p$ ;

$$\beta_1 = \frac{C_{ae}/C_c}{1 + C_r/C_c} \quad (5)$$

$$\beta_2 = C_{ae}/C_c \quad (6)$$

For Fucino clay, with  $C_{ae}/C_c = 0.042$  and  $C_r/C_c = 0.166$  and assuming, on the basis of geological evidence,  $64 \leq t/t_p \leq 150$ , one gets  $OCR_\alpha = 1.16$  to  $1.20$  and  $K_{o\alpha} = 0.76$  to  $0.84$ .

d. The values of  $K_o$  and OCR estimated above are in fair agreement with the results of oedometer tests and FVT's. It is worth observing that the values of  $OCR > OCR_\alpha$  obtained in the lower part of the investigated stratum (see Figure 6) can be attributed to interparticle bonding resulting from the abundant  $CaCO_3$  content. On the other hand, DMT's and SBPT's results suggest a more pronounced overconsolidation. The reasons of this disagreement are not easy to explain. The following points might be of interest, at least from a qualitative point of view:

- The values of  $\sigma'_p$  and OCR obtained from oedometer tests might be too low because of the unavoidable effect of sampling and of the uncertainty linked to the estimate of  $\sigma'_p$ .
- The correlations used to assess OCR and  $K_o$  from the results of DMT's have been validated in less structured clay deposits. Therefore, it cannot be excluded that the use of these correlations in the highly structured cemented Fucino clay might lead to overestimate the above mentioned stress history parameters.
- The values of  $K_o$  inferred from SPBT's are in perfect agreement with those obtained from DMT's. Two possible reasons for such unrealistically high values are given in the following: firstly, in cemented clays  $p_o$  might be an indicator of the yield stress at the expanding cavity wall, rather than the measure of the horizontal in situ stress. Secondly, the current  $u$  at the cavity wall could have been higher than the hydrostatic one,  $u_o$ , assumed in the calculations.

## 5 COMPRESSIBILITY, FLOW AND CONSOLIDATION

Compressibility characteristics of Fucino clay have been determined in the laboratory by means of conventional IL and CRS oedometer tests.

Figure 8 shows typical compression curves obtained by CRS tests, and Figure 9 summarizes all compression curves obtained by IL tests. The following observations can be drawn from these figures:

- all compression curves show a well defined yield stress  $\sigma'_p$ , which confirms that the sampling operations have not significantly altered the soil structure;
- at stresses immediately greater than  $\sigma'_p$ , compressibility increases abruptly showing a collapse in the soil structure;
- the compression index  $C_c$  is not constant, but decreases with vertical effective stress  $\sigma'_v$ . As shown in Figure 10, values of  $C_c$  range from 1.0-2.0 at vertical stresses immediately greater than  $\sigma'_p$ , to 0.6-0.7 for vertical stresses equal to 4-5 times  $\sigma'_p$ ;
- the lower values of  $C_c$ , corresponding to a destructured state, are in good agreement with empirical correlations (Terzaghi & Peck 1967) between  $C_c$  and  $w_L$  for reconstituted soil;

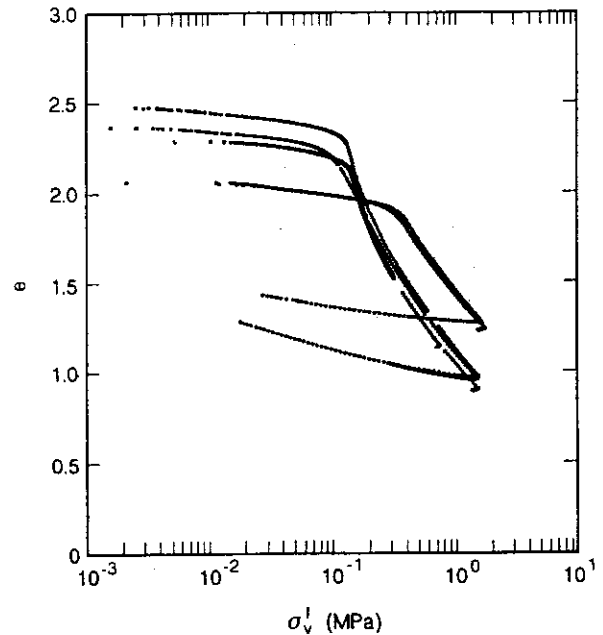


Figure 8. Typical compression curves from oedometer CRS tests.

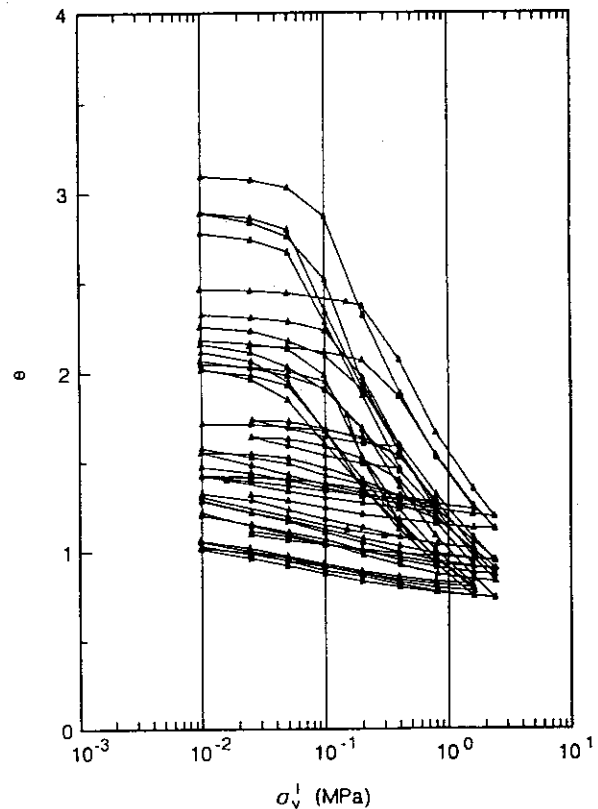


Figure 9. Typical compression curves from oedometer IL tests.

- values of the swelling index  $C_s$  vary between 0.13 and 0.15 in the upper 25 m, and between 0.07 and 0.10 in the lower 15 m of the investigated stratum.

As recently proposed by Burland (1990), this kind of behaviour can be successfully interpreted by comparing compressibility curves of the clay in its

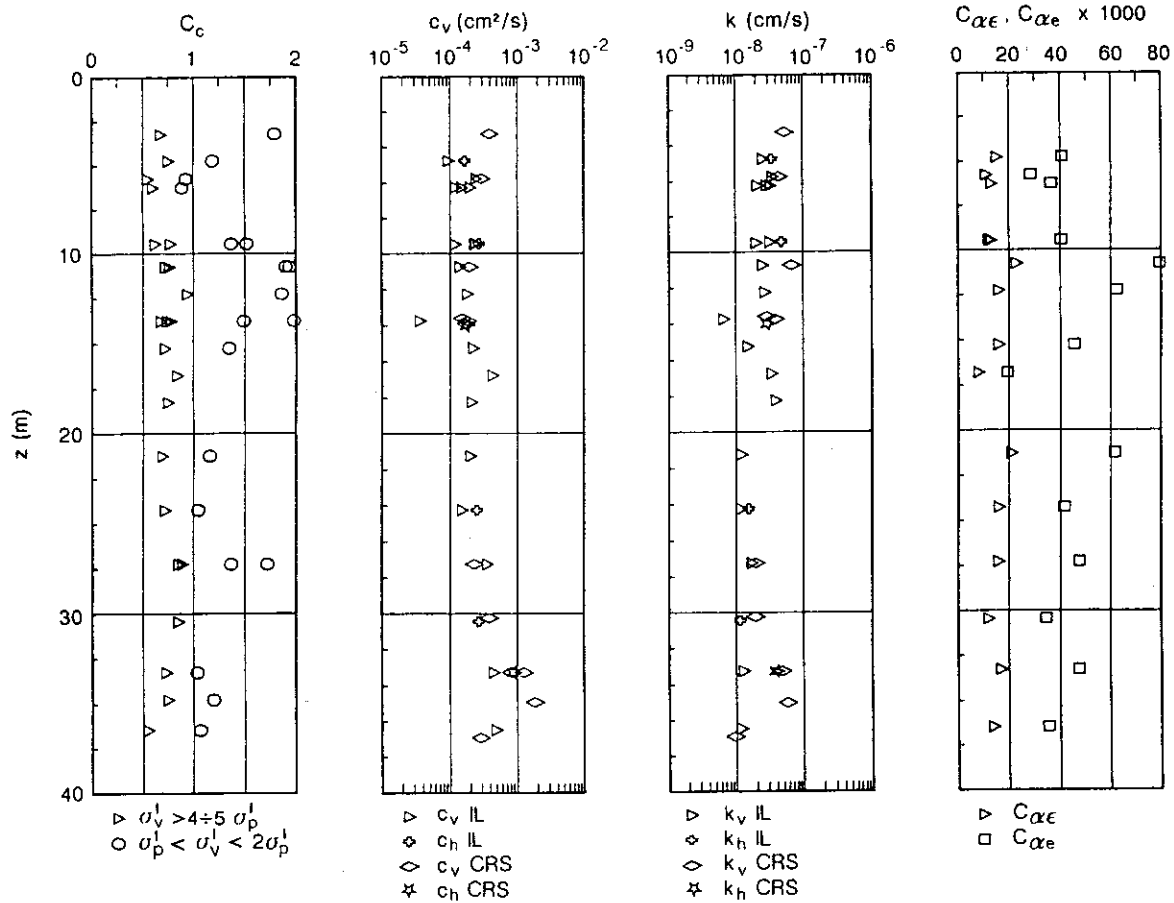


Figure 10. Compressibility, flow, and consolidation characteristics.

natural and reconstituted (intrinsic) states, previously normalized with respect to the void index  $I_v$  defined as:

$$I_v = \frac{(e - e_{100}^*)}{(e_{100}^* - e_{1000}^*)} = \frac{(e - e_{100}^*)}{C_c^*} \quad (7)$$

Following Burland's notation, an asterisk denotes an intrinsic property and  $e_{100}^*$ ,  $e_{1000}^*$  are the void ratios corresponding to  $\sigma_v' = 100$  kPa and 1000 kPa, respectively. These terms correspond to the notation used in the Critical State Soil Mechanics to define the virgin compression line. In order to evaluate the intrinsic properties of the clay, a CRS test was performed on a reconstituted sample, having an initial water content equal to  $1.5 w_L$ . The values of the intrinsic characteristics of compressibility ( $C_c^*$  and  $e_{100}^*$ ) thus obtained are in good agreement with the ones proposed by Burland (1990) by means of empirical correlations with the Atterberg limits.

Figure 11 shows the sedimentation compression curve of Fucino clay, together with the intrinsic compression line (ICL) and the sedimentation compression line (SCL) proposed by Burland. It is noted that the sedimentation curve has the typical saw-tooth shape and lies well above the SCL. This finding is explained by the cementation resulting from  $\text{CaCO}_3$  content.

The effect of cementation on compressibility can be observed by plotting the oedometer tests on natural samples in terms of void index  $I_v$ , as shown in Figure 12; the application of a load beyond  $\sigma_p'$  causes a progressive disruption of interparticle bonding. After yielding, the compression curves are considera-

bly steeper than the SCL, intersect the SCL from above and then flatten. At high pressures, the curves converge to the ICL and compressibility seems to slowly decrease to the value of the intrinsic compression index  $C_c^*$ .

A few oedometer IL tests were performed on horizontally trimmed specimens; typical results are shown in Figure 13, where two specimens trimmed in horizontal and vertical directions from the same

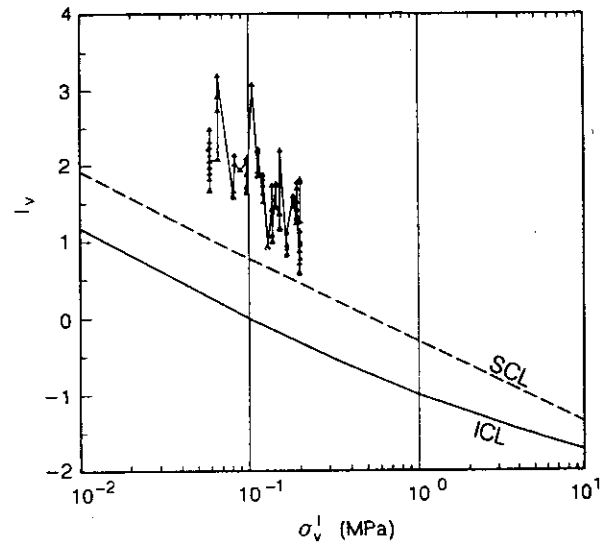


Figure 11. Sedimentation compression curve of Fucino clay with ICL and SCL lines.

sample are compared. It is observed that the behaviour of the two specimens is quite similar.

Flow and consolidation characteristics of Fucino clay have been evaluated in the laboratory by means of oedometer IL and CRS tests, and permeability flow-pump tests.

Values of the coefficient of consolidation for vertical flow,  $c_v$ , have been estimated by means of Casagrande's method from conventional IL tests, and by means of Wissa et al. (1971) [modified by Lee (1981)] method from CRS tests. They are plotted with depth in Figure 10; these values were obtained at effective stresses equal to twice the yield stress.

Coefficients of vertical permeability,  $k_v$ , have been directly measured in the flow-pump test, and back-calculated from  $c_v$  values obtained by IL and CRS tests (Desideri 1989). The results are collected in Figure 14, where  $k_v$  values are plotted against void

ratio. It is worth noting the good agreement between the values of  $k$  obtained by flow-pump and CRS tests; as previous experimental data indicate, an approximately linear relationship between  $\log k$  and  $e$  is obtained. On the other hand, the values of  $k$  back-calculated from standard IL tests show considerable scatter.

The effect of structure on flow characteristics is

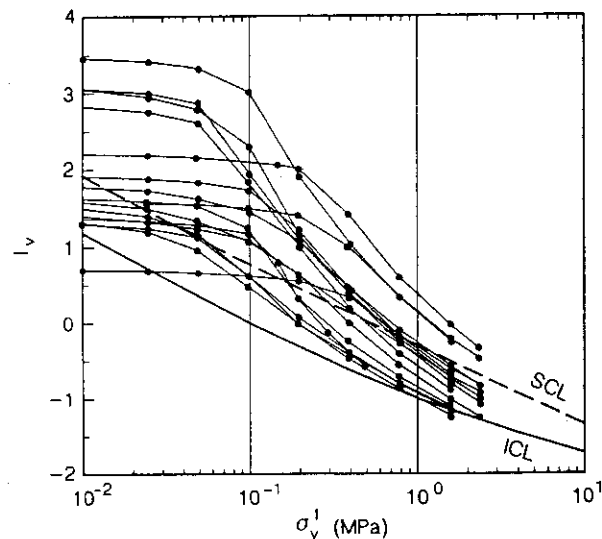


Figure 12. Compression curves in terms of void index  $I_v$ .

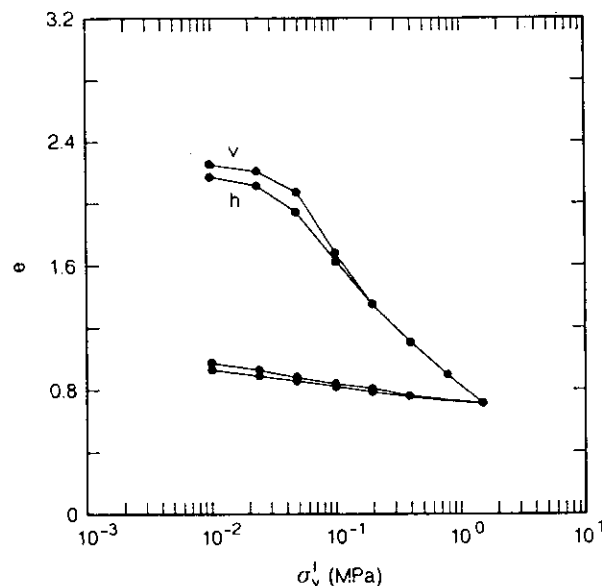


Figure 13. Oedometer curves for specimen trimmed in horizontal (h) and vertical (v) directions.

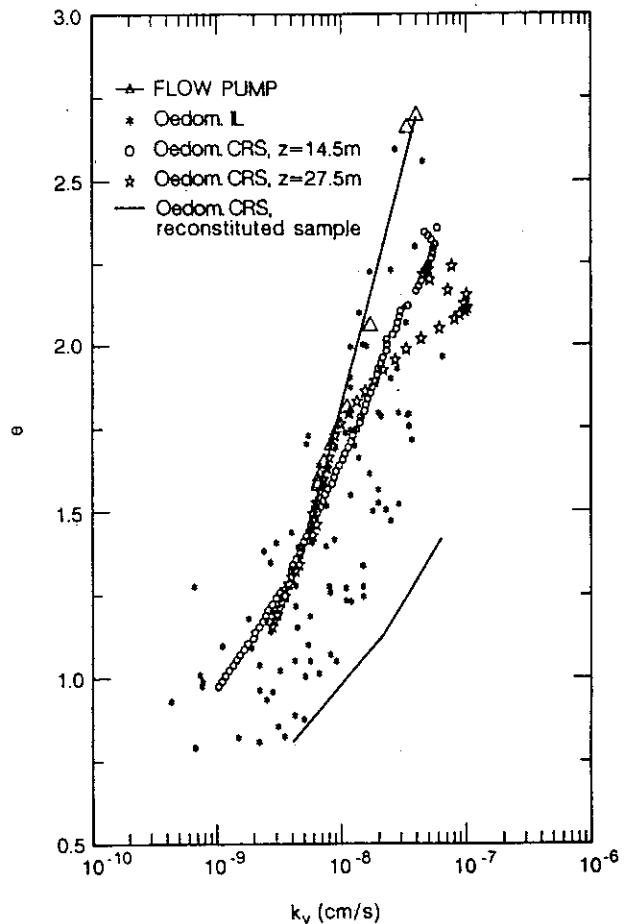


Figure 14. Coefficient of permeability for vertical flow from different tests.

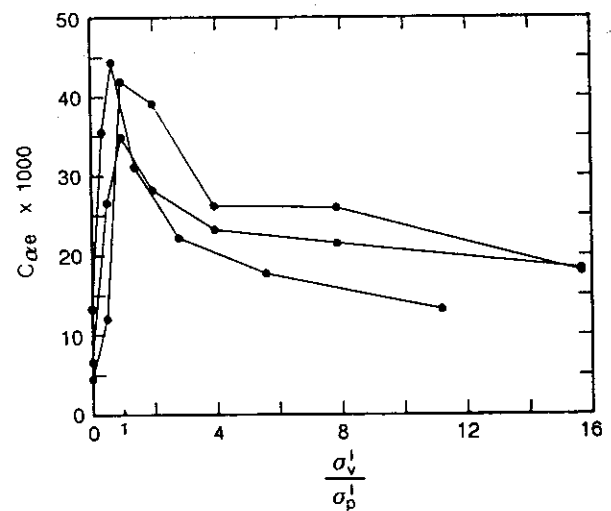


Figure 15. Coefficients of secondary consolidation  $C_{\alpha e}$  against normalized vertical effective stress.

depicted in Figure 14, which shows void ratio-permeability relationships for natural and reconstituted states. It is worth observing that the permeability of the natural soil is 5-10 times lower than the one of the reconstituted soil.

Only a few tests were carried out on horizontally-trimmed specimens; although limited in number, these tests seem to indicate that the ratio between horizontal and vertical permeabilities is less than 1.5.

With regard to creep characteristics, values of the coefficient of secondary consolidation  $C_{\alpha e}$  are plotted against vertical effective stress in Figure 15; it is observed that  $C_{\alpha e}$  increases significantly at stresses below the yield stress  $\sigma'_p$ , as expected.

Profiles of  $k$ ,  $C_{\alpha e}$  and  $C_{\alpha c}$  for the deposit, obtained at effective stresses equal to twice the yield stress, are shown in Figure 10.

## 6 SOIL STIFFNESS

It is well recognized that the stiffness of natural soils at relatively small strain levels represents an important parameter in geotechnical design.

The stiffness of Fucino clay at low-intermediate strain levels ( $10^{-6}$ - $10^{-3}$ ) has been investigated in situ by means of seismic tests and in the laboratory by means cyclic/dynamic torsional shear tests.

### 6.1 Seismic in situ tests

Seismic in situ testing inherently provides the best estimate of shear stiffness at low shear strain levels ( $<10^{-5}$ ). In fact, their execution is not affected by the unavoidable drawbacks arising from sampling disturbance and macrostructure effects.

Different testing procedures were used at Fucino site, by the research teams involved.

Two Cross-Hole (CH) and one Down-Hole (DH) tests were carried out by the Geotechnical Engineering Department of the University of Naples. Furthermore, two CH and one DH tests were performed by ISMES using the Seismic Cone (SC) device.

The main differences between the two kinds of CH and DH configurations are related to the features of impulsive sources and receivers used. The University of Naples CH source is an in-hole shear hammer clamped to the side-wall, while the DH source is an aluminium plate coupled to ground surface by steel studs. The receivers consist in 3-directional geophones, clamped to the borehole casing via a pneumatic membrane. Each receiver is provided by 3 miniature differential amplifiers directly positioned on the top of the geophones (Mancuso et al. 1988).

In the seismic cone configuration, the CH shear waves source is a friction bearing cone and the 3-D receiver is inside a second friction bearing cone (Baldi et al. 1988).

In addition to CH and DH tests, two SASW (Spectral Analysis of Surface Waves) tests were carried out by the geotechnical team of the University of Texas at Austin. The SASW method is a recently developed technique allowing a reliable identification of shear wave velocity profiles through analysis of Rayleigh surface waves characteristics (Nazarian & Stokoe 1985; Rix 1988).

Independently from the testing procedure a value of 1500 m/s was measured for the P-wave velocity,  $V_p$ , i.e., the value of  $V_p$  in water. This confirms that the degree of saturation in situ is very close to

100%. Therefore in the following only shear wave velocity profiles will be considered.

### a. Single receiver CH and DH tests

**Cross-Hole.** In Figure 16 results obtained from classical (CH) and seismic cone (SC) tests are compared. Since the latter were performed using one receiver, both data sets are in terms of direct shear wave velocities (i.e. derived from the SV-wave travel time, given by the difference between the initial arrival time at the receiver and the wave starting time at the source). Despite the considerable differences in the experimental configurations, the results are in fairly good agreement.

**Down-Hole.** Both ISMES and University of Naples DH data refer to initial arrival times of SH-wave. Due to the simple geometric patterns assumed for the processing criteria of field data, shear wave velocity profiles from DH tests are generally considered less accurate than those evaluated by CH tests. To improve the quality of the results, the University of Naples has used a recently developed inversion procedure (Mok 1987; Stokoe et al. 1989). Figure 16 shows velocity profiles inferred from the initial arrival times obtained by SC (triangles) and from the above mentioned DH inversion procedure (solid line). Again, in spite of the inherent differences existing between the two experimental configurations and interpretation procedures, the results are in fairly good agreement.

### b. Multiple receiver CH tests

The use of two or more receivers provides more reliable results, since the corresponding  $V_s$  values are less affected by experimental error and subjective interpretation.

With the conventional visual analysis, a two-receiver record allows to recognize further typical wave points, as peaks and troughs; hence several interval velocities ( $V_1, \dots, V_n$ ) can be obtained. At Fucino, it was often observed (Mancuso et al. 1989) a marked decrease of shear wave velocity values from the first arrival time to the last peak or trough ( $V_n/V_0$  even lower than 0.85).

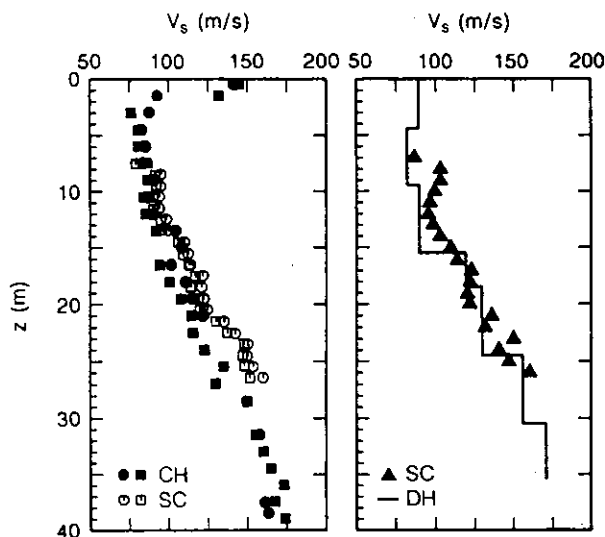


Figure 16. Shear wave velocities derived from CH (left) and DH (right) tests using one receiver.



This phenomenon (known as spreading) is caused by larger losses of energy related to higher frequency components of the signal; wave-forms change their shapes during propagation, increasing the time interval between peaks and troughs. The effect of spreading on low strain shear modulus ( $\alpha V_s^2$ ) is even more important.

The use of numerical analysis procedures allows an objective estimate of mean wave-form velocity. In this research project, two completely independent numerical procedures were used, that is, cross-correlation and cross-power spectrum. They allow to define the cross-correlation velocity ( $V_{cc}$ ) and group velocity ( $V_g$ ) (Mancuso et al. 1989), which are both a convenient representation of the overall wave propagation in the subsoil. From the values plotted in Figure 17, it is clear that the above techniques give approximately the same results.

### c. Spectral analysis of surface waves (SASW)

In the SASW method, by using properly selected data from different receiver spacings, it is possible to construct a plot of the velocity of each frequency component of the signal (phase velocity) versus its wave-length (raw dispersion curve). The final dispersion curve is then obtained on the basis of statistical calculations at each wave-length (Nazarian & Stokoe 1986). To determine the actual shear velocity profiles, an inversion process of the dispersion curve is then required; this is an interactive procedure to fit the experimental data with the response of a theoretical model.

In Figure 17, the shear wave velocities derived from SASW ( $V_{SASW}$ ) are compared with the ones derived from cross-correlation ( $V_{cc}$ ) and cross-power spectrum ( $V_g$ ) numerical techniques. The values are in good agreement, thus confirming that  $V_{cc}$ ,  $V_g$  and  $V_{SASW}$  represent the best estimate of shear wave-forms velocities.

## 6.2 Laboratory tests

In this research project, a considerable effort was concentrated in the evaluation of the stress-strain response of Fucino clay by torsional shear tests (Pane & Burghignoli 1988).

The tests were performed both in dynamic (resonant column, RC) and quasi-static (cyclic torsional shear, TS) loading conditions by means of the same device, originally designed at the University of Texas at Austin (Isenhour 1979).

The non-destructive nature of the low-amplitude RC tests allows to evaluate on a single specimen the variability of  $G_0$  throughout a wide range of consolidation pressures. The dependence of  $G_0$  on the current state of the soil (namely, mean effective stress  $p'$ , OCR, void ratio) has been longely recognized as an essential feature of soil behaviour (Hardin 1978).

Moreover, the wide range of frequencies (from 0.01 Hz to about 100 Hz) that can be used during an RC-TS test on the same specimen allows to investigate the strain rate effect.

In order to evaluate the stiffness properties of Fucino clay, 12 specimens were trimmed from undisturbed samples recovered from depths ranging between 3 and 37 m.

The experimental program implied a series of isotropic consolidation stages on each specimen, at increasing values of the consolidation stress  $p'$ . For all specimens, the maximum value of  $p'$  was greater than the estimated in situ mean effective stress  $p'_0$ .

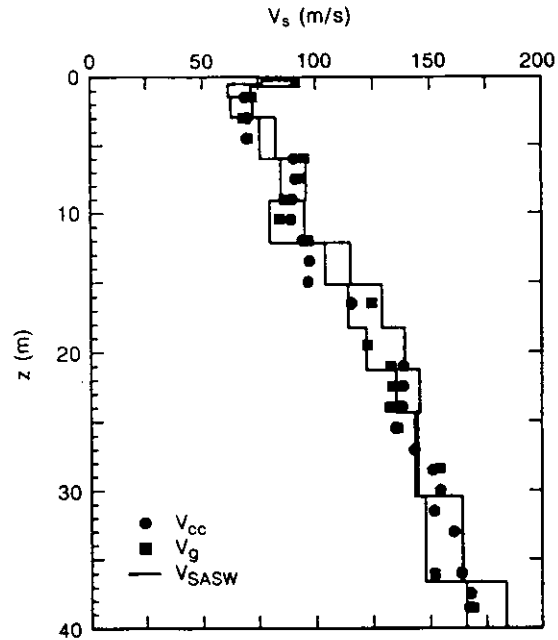


Figure 17. Comparison between shear wave velocities derived by means of numerical analysis of CH and SASW data ( $V_{cc}$ ,  $V_g$  and  $V_{SASW}$ ).

At each  $p'$  the low-amplitude shear modulus  $G_0$  was measured by means of RC tests at  $\gamma < 10^{-5}$ . Thereafter, the high amplitude test series was performed; at each strain level a set of three TS tests at increasing frequencies (namely 0.0067 Hz, 0.067 Hz and 0.67 Hz) was run. Afterwards, the high amplitude resonant test was carried out.

In the following, the tests results will be presented and discussed, taking separately into account the effects of consolidation stress, shear strain and strain rate.

### a. Dependence of initial stiffness on $p'$

$G_0$  is usually expressed as a function of mean effective stress  $p'$ , void ratio  $e$ , and overconsolidation ratio OCR. However, if the soil is normally consolidated, an unique relationship exists between void ratio and mean effective stress. For a given normally consolidated soil, a correlation expressing the dependence of  $G_0$  from the state parameters can be expressed as:

$$G_0 = a (p')^n \quad (8)$$

For cohesive soils the parameters  $a$  and  $n$  of this empirical equation can be associated to mineralogical and micro-structural features of the soil skeleton (Hardin 1978).

Figure 18 shows the variation of  $G_0$  for values of the consolidation stress  $p' = p'_0$ . The distinction is made between specimens taken in the upper part ( $10\% < \text{CaCO}_3 < 30\%$ ) and in the lower part ( $\text{CaCO}_3 = 60\%$ ) of the explored stratum. The influence of  $\text{CaCO}_3$  content on the measured  $G_0$  values is evident.

The next Figure 19 reports the values of  $G_0$  obtained from RC tests on specimens consolidated beyond the preconsolidation mean effective stress in situ,  $p'_p$ .

### b. Dependence of shear stiffness on shear strain

In Figure 20, the shear moduli measured in RC tests

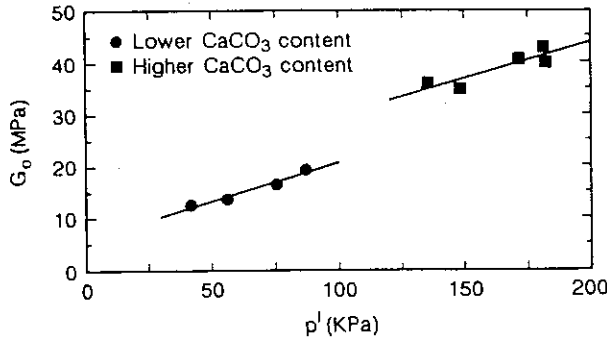


Figure 18. Effect of  $\text{CaCO}_3$  content on  $G_0$  resulting from RC tests at  $p' = p'_0$ .

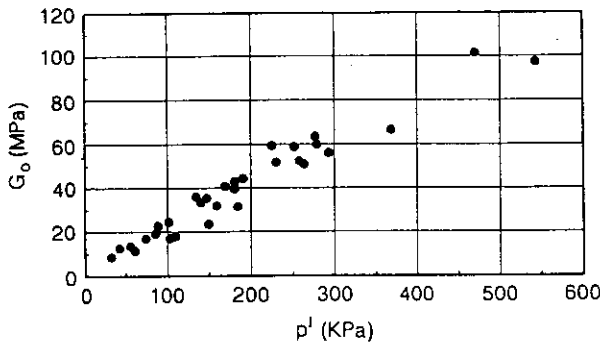


Figure 19. Values of  $G_0$  obtained from RC tests at  $p' > p'_0$ .

at strains larger than  $10^{-5}$ ,  $G_{RC}$ , have been normalized with respect to the initial moduli  $G_0$  and plotted as a function of  $\gamma$ . Although the data points pertain to a wide range of consolidation stresses ( $50 < p' < 500$  kPa), the results define, within a narrow band, the strong dependence of  $G$  upon strain level.

A noticeable decay of  $G(\gamma)$  occurs beyond a threshold shear strain of about  $10^{-4}$ . No appreciable effect of consolidation stress level on the shape of the normalized curve is noticed.

The trend of  $G(\gamma)$  is consistent with the one encountered in other medium to high plasticity clays (Isenhower 1979, Saada and Macky 1985, Dobry and Vucetic 1987, Lo Presti 1989).

The whole set of data in Figure 20 can be well fitted by means of the Ramberg-Osgood back-bone curve (1943).

#### c. Dependence of shear stiffness on strain rate

Typical results showing the frequency ( $f$ ) dependence of  $G_0$  of Fucino clay is shown in Figure 21a. For harmonic loading the mean shear strain rate  $\dot{\gamma}$  can be approximately expressed by  $\dot{\gamma} = 4\gamma f$ . Hence, in order to deduce the shear strain-rate effect on stiffness, it is necessary to plot the  $G$  values obtained, at constant  $\gamma$  against  $f$ , as shown in Figure 21b. The increase of  $G$  per logarithmic cycle of  $\dot{\gamma}$  is about 5%, regardless the values of consolidation stress and strain level.

#### 6.3 In situ versus laboratory stiffness measurements

In situ shear moduli  $G_0$  derived from cross-correlation and group velocity techniques are plotted in

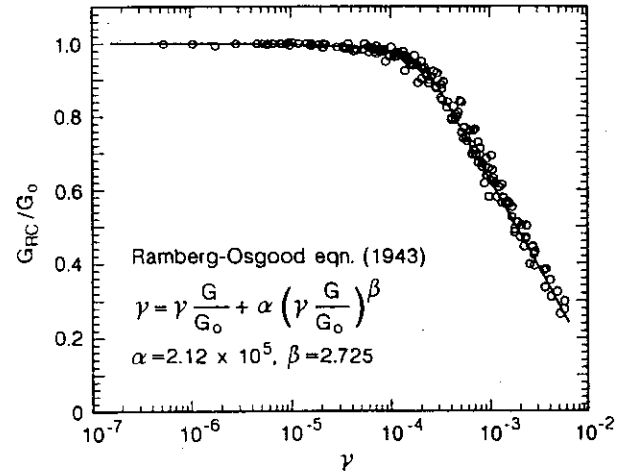


Figure 20. Dependence of shear stiffness on shear strain level.

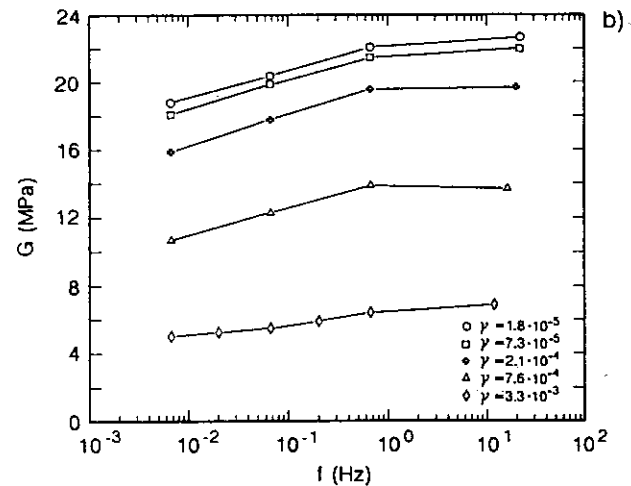
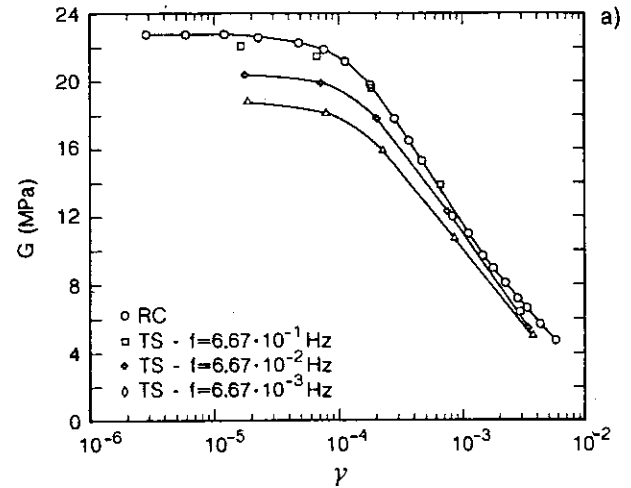


Figure 21. Dependence of shear stiffness on shear strain rate.

Figure 22. These values can be significantly compared with those derived from RC tests (Figure 18), properly converting depth into  $p'_0$ .

Despite the inherent differences of both experimental procedures and interpretation criteria, a very close agreement is obtained between laboratory and in

situ measurements. This unusual situation might be attributed to the existence of cementation, to the lack of relevant macrostructure characteristics, and to the use of reliable experimental techniques (high quality of undisturbed specimens, analog and digital filtering, numerical processing criteria).

The results of the in situ seismic tests shown in Figure 22 reveal an increase of initial shear stiffness below a depth of 20 m. Such occurrence is probably related to the difference in  $\text{CaCO}_3$  content and the resulting cementation.

Table I reports some examples of the unload-reload shear stiffness  $G_{ur}$  measured during the SBPT's.

The values of  $G_{ur}$  have been obtained at:

- Values of  $p_{max}$  appreciably higher than the cavity yield stress, equal to  $2 c_u$ .
- Values of shear strain at the cavity wall,  $\Delta\gamma$ , varying between  $1.8$  and  $2.8 \cdot 10^{-3}$ .

These values of  $\Delta\gamma$  are approximately twice the average shear strain in the plastic zone around the expanding cavity. Hence the measured  $G_{ur}$  corresponds to the shear stiffness at strain levels of the order of  $1 - 1.5 \cdot 10^{-3}$ .

Due to the large values of the total cavity stress at the start of the unloading loops, the  $G_{ur}$  values should be representative of destructured Fucino clay.

On average, the ratio between the values of  $G_{ur}$  and the values of  $G_o$  of the destructured Fucino clay (see Figure 19 for  $100 < p' < 150$  kPa) ranges between 0.4 and 0.5. It is worth noting that, according to Figure 20, these ratios correspond to shear strains of the order of  $2 \cdot 10^{-3}$ , i.e., comparable to the ones estimated above for the average strain around the expanding cavity.

Table I. Examples of unload-reload modulus from SBPT's.

Depth [m]	$G_{ur}$ [MPa]	$p_{max}^c$ [MPa]	$\Delta p^c$ [kPa]	$\Delta\gamma$
20	7.6	0.438	28	$2.8 \cdot 10^{-3}$
22	11.7	0.493	27	$2.3 \cdot 10^{-3}$
24	11.9	0.526	18	$2.5 \cdot 10^{-3}$
26	13.9	0.550	22	$1.7 \cdot 10^{-3}$
28	14.4	0.672	16	$1.8 \cdot 10^{-3}$
30	15.4	0.696	26	$1.7 \cdot 10^{-3}$

$p_{max}^c$  - total cavity stress at the start of unloading

$\Delta p^c$  - reduction of the total cavity stress during the loop

$\Delta\gamma$  - shear strain amplitude at the cavity wall

## 7 SHEAR STRENGTH

Shear strength characteristics of Fucino clay have been determined by means of field and laboratory tests.

The experimental data are summarized in Figure 23 which reports the variation of the undrained strength  $c_u$  with depth as inferred from laboratory tests, FVT's, SBPT's, DMT's, CPT's, and Piezocone (CPTU) tests.

The values of  $c_u$  (FVT) are not corrected as far as strain rate and anisotropy effects are concerned (see Bjerrum 1972 and 1973). The  $c_u$  values as resulting

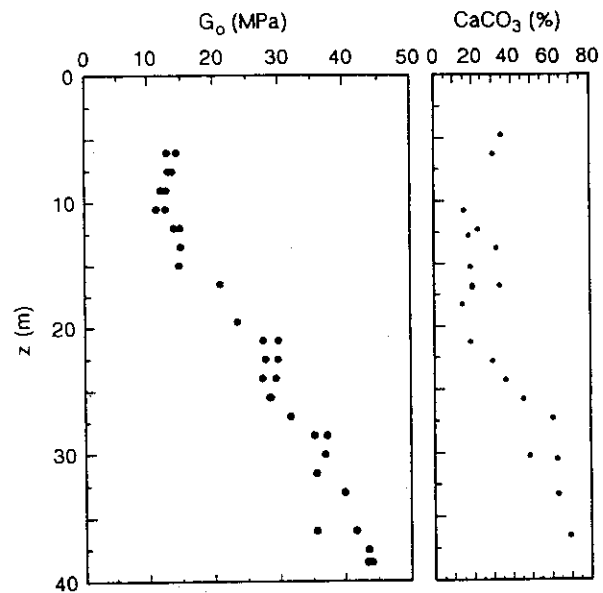


Figure 22. Initial Shear Modulus obtained from  $V_{cc}$  and  $V_g$  compared against  $\text{CaCO}_3$  content.

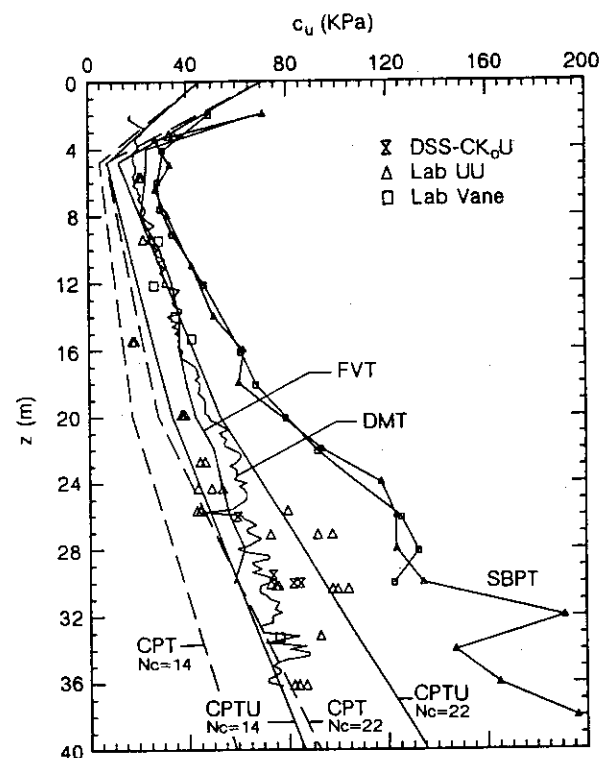


Figure 23. Undrained shear strength from laboratory and in situ tests.

from CPT's and CPTU's have been obtained assuming a cone bearing capacity factor  $N_c$  ranging between 14 and 22.

With reference to the various field test results, it is observed that below the upper desiccated crust there is a fair agreement between the  $c_u$  values resulting from FVT's and DMT's. The SBPT's lead to values of  $c_u$  significantly higher than those resulting from other in situ tests.

Figure 24 shows the values  $c_u$  as resulting from the unconsolidated-undrained triaxial compression tests

(UU) and from the DSS-CKoU tests. This figure indicates a marked increase of  $c_u$  below a depth of 20 to 25 m, reflecting the trend of  $\text{CaCO}_3$  content which changes with depth. This feature is not displayed by the results of in situ tests with the exception of SBPT's. In fact, only this field technique provides an indication of the differences in the undrained strength between upper and lower parts of the investigated clay thickness.

The above mentioned observations suggest that in highly structured soft clay deposits like Fucino clay the results of many field tests (e.g. CPT, DMT and to some extent FVT) can be hampered by the destructuration of the tested soil, induced by the insertion of the device. This might lead to an underestimate of the  $c_u$  from in situ test results.

As far as drained shear strength is concerned, some typical results of isotropically consolidated drained (CID) and undrained (CIU) triaxial compression tests are reported in the following for sake of completeness. The tests shown in Figure 25 were all performed on specimens trimmed from the same sample, recovered at a depth of 9 m. The specimens were isotropically consolidated to pressures considerably larger than the preconsolidation stress. Hence, the effective stress strength envelope in Figure 25 must be considered as representative for the destructured Fucino clay. It is worth observing in this figure the large axial deformations ( $\epsilon_a \approx 30\%$ ) necessary to reach failure during drained shearing; however, at these large deformations the experimental data are of difficult interpretation to the irregular barrel shape of tested specimens.

An overall observation of all triaxial tests carried out on normally consolidated destructured specimens leads to the following values of strength parameters:

$$c' = 0$$

$$\phi' = 29^\circ - 31^\circ$$

## 8 CONCLUDING REMARKS

The original aim of the investigation was to select a suitable deposit of soft and homogeneous clay, in order to carry out comparative in situ and laboratory tests. The choice fell on the Fucino testing site because of the marked spatial homogeneity, of the lack of an appreciable macrostructure, and of the apparently simple geological history. However, it was found that the clay possesses significant diagenetic bonds due to  $\text{CaCO}_3$  cementation which rendered the interpretation of various tests (especially the in situ ones) rather difficult and uncertain.

Some points of interest, as well as unanswered questions, arise from the results of the investigation. Despite its relatively recent deposition, the clay is highly structured and cemented. The most evident effect of cementation is in the values of the void ratio in situ; these values are well above the sedimentation compression line, i.e., they are considerably larger than the ones corresponding to the reconstituted clay, at a given vertical effective stress. Yielding, as observed in laboratory tests, is quite distinct, as well as post-yielding structure collapse.

The overconsolidated state of the clay is most likely due to aging and diagenetic bonds; this feature is better evidenced by laboratory oedome-

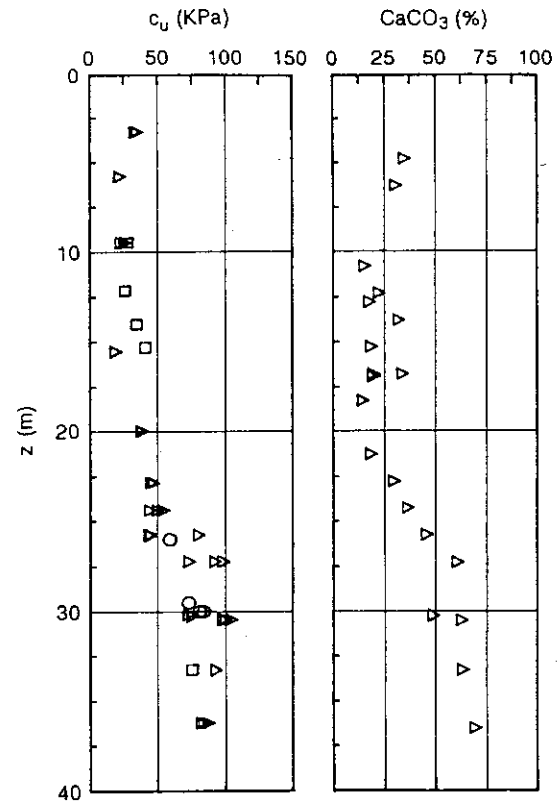


Figure 24. Undrained shear strength from laboratory tests and  $\text{CaCO}_3$  content.

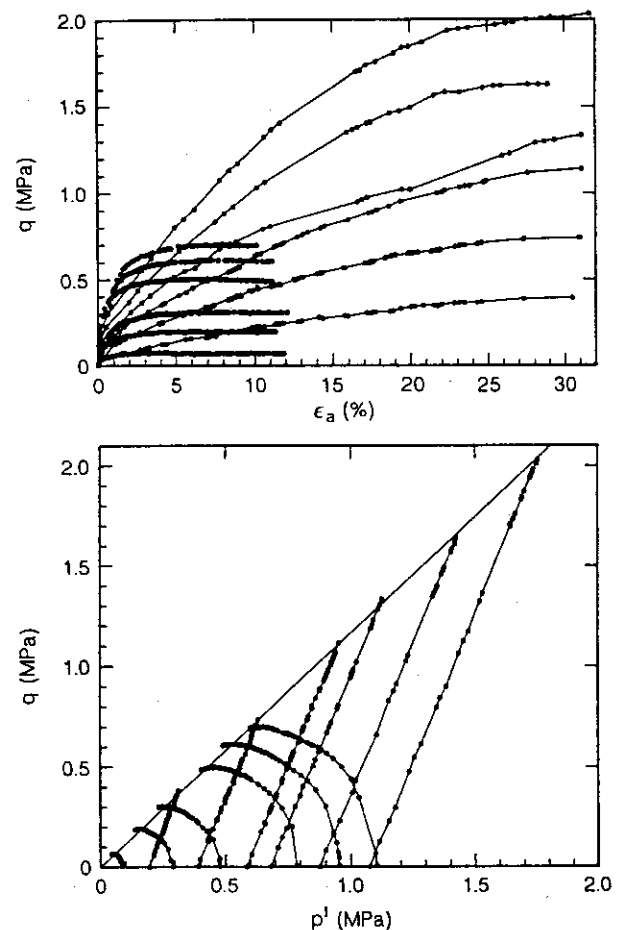


Figure 25. Typical results of CIU and CID triaxial compression tests.

ter tests, which also suggest a quantitative link between  $\text{CaCO}_3$  contents and the values of OCR. On the contrary, in situ (DMT and SBPT) tests do not reflect the variation of  $\text{CaCO}_3$  content with depth. Moreover, they seem to overestimate the OCR and  $K_0$  values of the deposit.

The dependence of undrained shear strength on  $\text{CaCO}_3$  content is better evidenced by UU triaxial compression tests and, partially, by the results of SBPT's. On the contrary, the large strains involved in the penetration of other in situ devices obliterate partially the effect of diagenetic bonds on the inferred undrained shear strength.

In this specific case, a good agreement is obtained between low-strain stiffness resulting from laboratory and seismic field tests. This occasional situation can be at least partially attributed to the existence of cementation, high quality of the undisturbed specimens used for laboratory tests, and to the lack of a significant macrostructure. In addition, the values of  $G_0$  resulting from both laboratory and in situ tests appear to be influenced by the  $\text{CaCO}_3$  content.

Hence, properly conducted laboratory tests and non-destructive field tests have provided useful tools in evaluation of the influence of fabric and interparticle bonding on the mechanical behaviour of a structured homogeneous Fucino clay deposit. On the other hand, the reported experimental data showed that lot of care must be devoted to the interpretation of in situ tests based on empirical correlations which have been validated in less structured materials.

#### ACKNOWLEDGEMENTS

We are grateful to Telespazio S.p.A. for providing the area pertaining to the investigation program and for the technical, logistical and organizational support kindly offered during the whole field testing period.

#### REFERENCES

- Baldi, G., Battaglio, M., Bruzzi, D., Jamiolkowski, M. & Superbo, S. 1988. Seismic Cone in Po River Sand. Proc. ISOPT-I, Orlando, Fla.
- Bjerrum, L. 1972. Embankments on Soft Ground. State-of-the-Art Report, Proceedings, ASCE Spec. Conf. on Performance of Earth and Earth-Supported Structures. Lafayette, Vol.2, pp.1-54.
- Bjerrum, L. 1973. Problems of Soil Mechanics and Construction on Soft Clays. State-of-the-Art Report, Session 4, Proceedings, VIII ICSMFE, Vol.3, pp.109-159.
- Burland, J.B. 1990. On the Compressibility and Shear Strength of Natural Clays. Rankine Lecture, Géotechnique, 40,3, pp.327-378.
- Desideri, A. 1989. Misura della conduttività idraulica delle argille. Riunione annuale dei ricercatori geotecnici, CNR, Roma.
- Dobry, R. & Vucetic, M. 1987. Dynamic Properties and Seismic Response of Soft Clay Deposits. Proc. Int. Symp. on Geotechnical Engineering of Soft Soils, Mexico City 2:51-87.
- Follieri, M., Magri, D. & Sadori, L. 1986. Late Pleistocene Zerkova Extinction in Central Italy. New Phytol., 103:269-273.
- Ghionna, V., Jamiolkowski, M., Lancellotta, R., Torrella, M.L. & Ladd, C.C. 1981. Performance of Self-Boring Pressuremeter Tests in Cohesive Deposits. MIT, Dept. of Civil Engineering.
- Giraudi, C. 1988. Evoluzione geologica della Piana del Fucino negli ultimi 30.000 anni. Il Quaternario, 1(2): 131-159.
- Hardin, B.O. 1978. The Nature of Stress-Strain Behaviour of Soils. Proc. Conf. Earthquake Engineering and Soil Dynamics, ASCE, Pasadena, California.
- Isenhower, W.M. 1979. Torsional Simple Shear/Resonant Column Properties of San Francisco Bay Mud. M.S. Thesis, University of Texas at Austin.
- Jamiolkowski, M., Ladd, C.C., Germaine, J. & Lancellotta, R. 1985. New Developments in Field and Laboratory Testing of Soils. Proc. XI ICSMFE, San Francisco.
- Kulhawy, F.H., Beech, J.F. & Troutman, C.H. 1989. Influence of Geologic Development on Horizontal Stress in Soil. Proc. Congress on Foundation Engineering: Current Principles and Practices, ASCE, Evanston Illinois.
- Lee, K. 1981. Consolidation with Constant Rate of Deformation, Géotechnique, Vol.31, pp.295-329.
- Lo Presti, D.C.F. 1989. Proprietà meccaniche dei terreni. Atti XIV Conferenze di Geotecnica di Torino.
- Mancuso, C., Simonelli, A.L. & Vinale, F. 1988. Misure di velocità delle onde di taglio nella piana del Fucino. CNR, Conv. Monselice (PD).
- Mancuso, C., Simonelli, A.L. & Vinale, F. 1989. Numerical Analysis of in Situ S-Wave Measurements. Proc. XII ISSMFE, June 1989, Rio de Janeiro.
- Marchetti, S. 1980. In Situ Testing by Flat Dilatometer. Journ. Geot. Eng., ASCE, N°3.
- Mesri, G. 1987. The Fourth Law of Soil Mechanics: The Law of Compressibility. Proc. of the Int. Symposium on Geotechnical Engineering of Soft Soils, Mexico City.
- Mesri, G. 1989. Personal communication to M. Jamiolkowski.
- Mok, Y.J. 1987. Analytical and Experimental Studies of Borehole Seismic Methods. Ph.D. Thesis, The University of Texas at Austin.
- Nazarian, S., Stokoe II, K.H. 1985. In Situ Determination of Elastic Moduli of Pavement System by Spectral Analysis of Surface Waves Method (practical aspects). R.R. n°368-1F, Center of Transp. Res., Bureau of Engineering Research, The University of Texas at Austin.
- Nazarian, S. & Stokoe II, K.H. 1986. In Situ Determination of Elastic Moduli of Pavement System by Spectral Analysis of Surface Waves Method (theoretical aspects). R.R. n°437-2, Center Transp. Res., Bureau Engineering Res., The University of Texas at Austin.
- Pane, V. & Burghignoli, A. 1988. Determinazione in laboratorio delle caratteristiche dinamiche dell'argilla del Fucino. CNR, Conv. Monselice (PD).
- Osterberg, J.O. 1973. An Improved Hydraulic Piston Sampler. VIII ICSMFE, Moscow, Vol.1-2, pp.317-321.
- Ramberg, W. & Osgood, W.R. 1943. Description of Stress-Strain Curves by Three Parameters. Technical note 902, National Advisory Committee for Aeronautics, Washington, D.C.
- Rix, G.J. 1988. Experimental Study of Factors Affecting the Spectral Analysis of Surface Waves Method. Ph. D. Thesis, The University of Texas at Austin.
- Saada, A.S. & Macky, T.A. 1985. Integrated Testing and Properties of a Gulf of Mexico Clay. Strength Testing of Marine Sediments: Laboratory and In Situ Measurements. ASTM STP833, Philadelphia.

- Serva, L., Blumetti, A.M. & Michetti, A.M. 1986. Gli effetti sul terreno del terremoto del Fucino (13/1/1915). Tentativo di interpretazione dell'evoluzione tettonica recente di alcune strutture. Mem. Soc. Geol. It., 35:893-907.
- Stokoe II, K.H., Mok, Y.J., Lee, N. & Lopez, R. 1989. In Situ Seismic Methods: Recent Advances in Testing, Understanding and Applications. Atti XIV Conf. Geotec., Torino.
- Terzaghi, K. & Peck, R.B. 1967. Soil Mechanics in Engineering Practice. II ed. John Wiley and Sons, New York.
- Wissa, A.E.Z., Christian, J.T., Davis, E.H., Heiberg, S. 1971. Analysis of Consolidation at Constant Strain Rate. Journal of the Soil Mech. and Foundation Division, Proceedings ASCE, Vol.97, No.SM10, October, pp.1393-1413.